Interfacial profiles in the rough phase

G. L. M. Dassen,* A. Kooiman, and J. M. J. van Leeuwen
Instituut-Lorentz, Nieuwsteeg 18, 2311 SB Leiden, The Netherlands

N. Jan
Physics Department, St. Francis Xavier University, Antigonish, Nova Scotia, Canada B2G 1C0
(Received 14 September 1989)

The interfacial profile of the order parameter is studied in the context of a d-dimensional Ising model by means of Migdal's renormalization procedure. It is found that interfaces between coexisting phases are always rough, such that pinning fields are necessary to locate and shape the interface. As a pinning field a linearly varying field (gravitational pinning) is taken, and scaling laws for the interface at criticality are established. In the low-temperature regime an interface is found that shows behavior similar to the capillary-wave model for low dimensions. Scaling forms are explicitly calculated.

INTRODUCTION

The study of the interfacial profile between two coexisting phases has a long tradition. Already, van der Waals[1] made a theory for the profile which now has been named the squared gradient theory. Subsequent sophistications of this theory all lead to a so-called intrinsic profile, i.e., a profile that is independent of the field that localizes its position. Buff, Lovett, and Stillinger[2] showed, however, that for dimensions $d \leq 3$ the interface is instable against capillary waves that are excited by thermal motion. As a consequence, the localizing field (e.g., gravity) also shapes the profile of the interface.

This result applies equally for lattices. In an Ising model the interface between a domain with positive magnetization and a domain with negative magnetization is rough for $d < 3$. In $d = 3$ the interface can be smooth (or intrinsic) below a critical temperature (the roughening temperature),[8] depending on the orientation of the normal of the interface.

In the rough phase the interfacial profile depends on the nature of the localizing field. Here we consider the case where the field that couples to the order parameter varies linearly in space (the gravitational situation). The interface then settles around the value of the field where the phase transition takes place, thus in the Ising model where the magnetic field is zero. The magnitude g of the gradient in the field then provides the scale or width of the interface. Capillary-wave theory[2] makes a definite prediction of the way g enters in the profile. The mean-squared displacement of the interface due to capillary waves diverges as $g^{(d-3)/2}$ for $d < 3$ and as $\ln g$ for $d = 3$. Consequently, the width of the interfacial profile diverges for small g and the profile itself becomes a function of $zg^{-(d-3)/4}$ for $d < 3$ and of $z/(\ln g)^{1/2}$ for $d = 3$, where z is the distance normal to the interface.

This behavior holds all along the coexistence line, but it changes over to critical behavior when the critical point is approached. In a varying field the interfacial width does not diverge as does the correlation length in the bulk, which is usually seen as a measure for the interfacial width. The interfacial profile is generally governed by scaling laws involving the bulk critical exponents.[3]

Few calculations of interfaces exist starting with the microscopic interaction between the constituent degrees of freedom which lead to the picture deduced from the semiphenomenological capillary-wave theory. In this paper we calculate the interface by real-space renormalization. The advantage is that such a calculation does not involve any ansatz on the behavior of the equation of state in the coexistence region which is a basic ingredient in the standard theory of the interface. The disadvantage is that the equations for the interface become quite involved when a reliable renormalization procedure is used. In this paper we use the Migdal procedure[4] in its continuous form, which has the virtue of great simplicity. Although limited to low dimensions, it still gives quite accurate results in $d = 2$ and more importantly the dimensional dependence can be obtained with d as a continuous parameter such that the behavior near $d = 1$, where the Migdal procedure becomes exact, can be analyzed.

The interface problem has been considered by various authors in the context of real-space renormalization.[5] The main effort has been to calculate the surface tension, which is left out in this paper, where the interfacial profile is the center of interest.

In Sec. I we provide the general real-space renormalization equations for an interface profile. In Sec. II the formulas for Migdal's renormalization procedure are given and applied to the calculation of the bulk magnetization. The equations from Migdal's scheme for the interface are derived in Sec. III. The solution is discussed in Sec. IV together with the numerical results for a number of cases. The paper closes with a discussion of the results and a comparison with the classical interface theories.

I. EQUATIONS FOR THE MAGNETIZATION

In the renormalization approach one studies the behavior of the system under a spatial rescaling. For the study of interfaces in the presence of an external varying field, the scaling behavior is more complicated. We consider an Ising system with the Hamiltonian

$$H[s_i]=\sum_i H_i s_i + K \sum_{\langle ij \rangle} s_i s_j \ . \tag{1.1}$$

The spin variables s_i assume the values $s_i=\pm 1$. H_i is the magnetic field on site i and we take a field H_i that is positive on one half of the lattice and negative on the other half, such that an interface is formed at the position where H_i changes sign. The direction perpendicular to the interface (referred to as longitudinal) is taken along the z axis. Thus a typical H_i is of the form

$$H_i = g z_i \ . \tag{1.2}$$

g plays the same role as the gravitational acceleration for fluid interfaces.

In (1.1) K couples nearest-neighbor spins $\langle ij \rangle$ and measures the temperature which is hidden in K [because throughout the paper $-(1/k_B T)$ is absorbed in the Hamiltonian]. Similarly, g contains a factor $-(1/k_B T)$, but we will vary the gradient of H_i to arbitrary (small) values such that we consider g as an independent variable even in the low-temperature limit $K \to \infty$.

A renormalization transformation maps $H[s_i]$ onto a new Hamiltonian $H'[s'_{i'}]$ of new spins $s'_{i'}$ on a new lattice with sites i'. The lattice distance of the new lattice in units of the old lattice distance is the spatial rescaling factor b. In general, $H'[s'_{i'}]$ will not be of the same simple structure as (1.1). It will contain, in addition to a magnetic field $H'_{i'}$ and a nearest-neighbor pair interaction K', all kinds of further ranged and multiple-spin interactions. In this paper we will avoid the appearance of these higher-order interactions by using Migdal's renormalization procedure. For the moment we include them under a general label $K_{\alpha i}$, where i refers to its location and α to the type of the interaction.

Thus we summarize the renormalization step by the set of equations

$$\begin{aligned} H'_{i'} &= H'_{i'}[H_i, K_{\alpha i}] \ , \\ K'_{\alpha i'} &= K'_{\alpha i'}[H_i, K_{\beta i}] \ , \end{aligned} \tag{1.3}$$

expressing that the new field $H'_{i'}$ at site i' depends, in principle, on all the fields H_i and coupling constants $K_{\alpha i}$ of the old system. We will assume, however, that the relations are nearly local, i.e., the field $H'_{i'}$ at site i' is mainly determined by the fields and couplings of sites i near the site i'.

The free energy of a system characterized by $H_i, K_{\alpha i}$ is a functional $F[H_i, K_{\alpha i}]$ and transforms under (1.3) as

$$F[H_i, K_{\alpha i}] = G[H_i, K_{\alpha i}] + F[H'_{i'}, K'_{\alpha i'}] \ , \tag{1.4}$$

where $G[H_i, K_{\alpha i}]$ is a spin-independent constant which is formed under renormalization. it could be considered as part of the Hamiltonian but it is usually treated separately because it plays no further role in the transformation (1.3).

The magnetization can be defined as

$$m_i = \delta F[H_i, K_{\alpha i}]/\delta H_i \ . \tag{1.5}$$

Variation of (1.4) with respect to the field H_i yields

$$m_i = \frac{\delta G}{\delta H_i} + \sum_{i'} \left[m'_{i'} \frac{\delta H'_{i'}}{\delta H_i} + \sum_\beta e'_{\beta i'} \frac{\delta K'_{\beta i'}}{\delta H_i} \right] . \tag{1.6}$$

$e_{\alpha i}$ is the abbreviation of the derivative

$$e_{\alpha i} = \delta F / \delta K_{\alpha i} \ . \tag{1.7}$$

When $K_{\alpha i}$ is a nearest-neighbor interaction, $e_{\alpha i}$ is the average of the product of a pair of nearest-neighbor spins.

Equation (1.6) shows that the equation for the magnetization has to be supplemented with an equation for $e_{\alpha i}$, which follows by variation of (1.4) with respect to $K_{\alpha i}$

$$e_{\alpha i} = \frac{\delta G}{\delta K_{\alpha i}} + \sum_{i'} \left[m'_{i'} \frac{\delta H'_{i'}}{\delta K_{\alpha i}} + \sum_\beta e'_{\beta i'} \frac{\delta K'_{\beta i'}}{\delta K_{\alpha i}} \right] . \tag{1.8}$$

The derivatives in (1.6) and (1.8) follow from the renormalization transformation (1.3) and the expression for $G[H_i, K_{\alpha i}]$.

Equations (1.6) and (1.8) express the set $\{m_i, e_{\alpha i}\}$ in terms of the set $\{m'_{i'}, e'_{\alpha i'}\}$ for the renormalized system and the derivatives of G. Repeated renormalization generally leads to an extreme situation: very weakly coupled systems (high temperatures) or very strongly coupled systems (low temperatures). In these extreme situations $\{m_i, e_{\alpha i}\}$ must be determined directly from the Hamiltonian. We will refer to these values as boundary conditions. Then, running the renormalization backwards to the original system, the values of $\{m_i, e_{\alpha i}\}$ for the original system can be calculated from repeated use of (1.6) and (1.8).

To elucidate the equations we may apply them to the homogeneous case $H_i = H$ and $K_{\alpha i} = K_\alpha$ such that we can drop the index i and the summation over i. The transformation (1.3) simplifies to

$$\begin{aligned} H' &= H'(H, K_\alpha) \\ K'_\alpha &= K'_\alpha(H, K_\beta) \ . \end{aligned} \tag{1.9}$$

The derivatives of (1.9) are related to the functional derivatives in (1.6) and (1.8) by the rules

$$\begin{aligned} \frac{\partial H'}{\partial H} &= \sum_i \frac{\delta H'_{i'}}{\delta H_i}, \quad \frac{\partial H'}{\partial K_\alpha} = \sum_i \frac{\delta H'_{i'}}{\delta K_{\alpha i}} \ , \\ \frac{\partial K'_\alpha}{\partial H} &= \sum_i \frac{\delta K'_{\alpha i'}}{\delta H_i}, \quad \frac{\partial K'_\alpha}{\partial K_\beta} = \sum_i \frac{\delta K'_{\alpha i'}}{\delta K_{\beta i}} \ . \end{aligned} \tag{1.10}$$

If we vary, e.g., H in (1.9), we vary all the H_i at the same time and the effect is in the homogeneous case independent of the location i' of $H'_{i'}$. The transformation laws for m and e_α follow from (1.6) and (1.8) by summation of all sites i and realizing that the number of sites N in the old lattice equals $b^d N'$ with N' the number of sites in the new lattice

$$b^d m = N'^{-1}\frac{\partial G}{\partial H} + m'\frac{\partial H'}{\partial H} + \sum_\beta e'_\beta \frac{\partial K'_\beta}{\partial H}$$
$$b^d e_\alpha = N'^{-1}\frac{\partial G}{\partial K_\alpha} + m'\frac{\partial H'}{\partial K_\alpha} + \sum_\beta e'_\beta \frac{\partial K'_\beta}{\partial K_\alpha} \quad . \tag{1.11}$$

From these relations the bulk magnetization $m(H,K_\alpha)$ may be derived in the same spirit. Starting from a set H,K_α apply the renormalization (1.9) repeatedly until an extreme situation is reached for which m and e are known. Then role back the renormalization trajectory and apply (1.9) until the original system is reached again. Thus the bulk equation of state $m_b(H,K_\alpha)$ is found.

II. MIGDAL TRANSFORMATION

In Fig. 1 we have drawn a $b\times b$ section (for $b=3$) of a $d=2$-dimensional lattice. The idea is to eliminate the spins that are not on the corners. In Migdal's approximation this is done by shifting the couplings between the pairs in the interior to the edges. This increases the couplings on the edges by a factor b^{d-1}. With only couplings on the edges, the spins in the interior can be eliminated as isolated spins and the spins on the edges can be eliminated as part of a one-dimensional chain. Thus an effective coupling results between the corner sites. When a magnetic field is present one can either shift the fields together with the bonds or leave the fields on the sites. Although the former procedure is more accurate near the critical point than the latter, we will choose in this paper for not moving the fields because it gives a better flow in the high-temperature regime, which is important for the boundary conditions.

An attractive feature of Migdal's renormalization technique is that it has quite simple renormalization equations and that it can be carried out for arbitrary dimension d and arbitrary rescaling factor b. This last point turns out to be very important for our renormalization flow equations for the magnetization. In fact, any integer b introduces inhomogeneities between sites which are eliminated and those which are kept. Therefore we will use the continuous form of the Migdal scheme and set $b=1+dt$ with $dt\to 0$. Then the equivalence of all sites remains unimpaired.

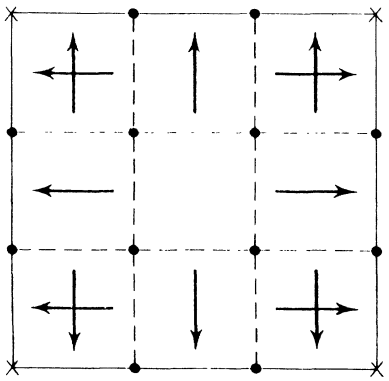

FIG. 1. Bond shifting in Migdal's approximation.

In this section we collect the formulas for the homogeneous case. In Sec. III the inhomogeneous case is treated.

The shifting of the interior bonds to the edges produces on the edges a bond strength

$$K_e = b^{d-1}K \quad . \tag{2.1}$$

The elimination of the sites along the edges leads to the problem

$$\exp[g + H_d(s+s') + K'ss'] = \sum_{\{s_1,\ldots,s_{b-1}\}} \exp[H(s_1+\cdots s_{b-1}) + K_e(ss_1+\cdots s_{b-1}s')] \quad . \tag{2.2}$$

The expressions for g, H_d, and K' in terms of H and K_e can be readily evaluated for arbitrary b by the transfer matrix method. For the reader's convenience we have worked out the general expression in the appendix. For $b\to 1$, we have to order $b-1=dt$,

$$\begin{aligned} g &\simeq \dot g(H,K)dt \quad , \\ H_d &\simeq \dot H(H,K)dt \quad , \\ K' &\simeq K + [(d-1)K + \dot K(H,K)]dt \quad , \end{aligned} \tag{2.3}$$

with $\dot g$, $\dot H$, and $\dot K$ given below, using (2.1) in the last equation.

The new field H' on the corner sites is given by

$$H' = H + 2dH_d \simeq H + dt\frac{\partial H}{\partial t} \quad . \tag{2.4}$$

We arrive at the following flow equations:

$$\begin{aligned} \frac{\partial H}{\partial t} &= 2d\dot H(H,K) \quad , \\ \frac{\partial K}{\partial t} &= (d-1)K + \dot K(H,K) \quad . \end{aligned} \tag{2.5}$$

The "time" t measures the scale along the renormalization trajectory. The relation $N=b^dN'$ between original and renormalized number of sites becomes, in continuous form,

$$N(t) = e^{-dt}N \quad , \tag{2.6}$$

where $N(t)$ gives the number of sites at time (or scale) t and N the starting number of sites.

The functions $\dot g$, $\dot H$, and $\dot K$ derived in the appendix are given by the following expressions:

$$\begin{aligned} \dot g(H,K) &= K + \tfrac{1}{2}\ln(1-e^{-4K}) + (\coth 2K)U(H,K) \\ \dot H(H,K) &= (\tanh H)U(H,K) \\ \dot K(H,K) &= -U(H,K) \quad , \end{aligned} \tag{2.7}$$

with $U(H,K)$ given by

$$\begin{aligned} U(H,K) &= \frac{1-e^{-4K}}{4q(H,K)}\ln\frac{1+q(H,K)}{1-q(H,K)} \quad , \\ q(H,K) &= [\tanh^2 H + e^{-4K}(1-\tanh^2 H)]^{1/2} \quad . \end{aligned} \tag{2.8}$$

The next step is to construct the flow equations for the magnetization from the general expressions (1.11). We observe first that only nearest-neighbor couplings play a role and thus the sum in (1.11) over the type α runs only through the d orientations of the bonds. In the homogeneous case all d orientations are equivalent and for each of them the second equation (2.5) applies individually. The function G in (1.11) is built up from d chains per new site. So for $b \to 1$

$$N'^{-1}G = d\dot{g}(b-1) = d\dot{g}\,dt \ . \tag{2.9}$$

We can calculate the derivatives in (1.11) from (2.5) and (2.9) for $dt \to 0$ as

$$\begin{aligned} &\frac{1}{N'}\frac{\partial G}{\partial H} = d\frac{\partial \dot{g}}{\partial H}dt, \quad \frac{1}{N'}\frac{\partial G}{\partial K_\alpha} = \frac{\partial \dot{g}}{\partial K}dt \ , \\ &\frac{\partial H'}{\partial H} = 1 + 2d\frac{\partial \dot{H}}{\partial H}dt, \quad \frac{\partial H'}{\partial K_\alpha} = 2\frac{\partial \dot{H}}{\partial K}dt \ , \\ &\frac{\partial K'_\beta}{\partial H} = \frac{\partial \dot{K}}{\partial H}dt, \quad \frac{\partial K'_\alpha}{\partial K_\beta} = \delta_{\alpha\beta}\left[1 + d - 1 + \frac{\partial \dot{K}'}{\partial K}dt\right] . \end{aligned} \tag{2.10}$$

For the values of m' and e' we put

$$\begin{aligned} m' &= m + \frac{\partial m}{\partial t}dt \ , \\ e' &= e + \frac{\partial e}{\partial t}dt \ . \end{aligned} \tag{2.11}$$

Inserting (2.10) and (2.11) into (1.11) yields for $dt \to 0$,

$$\begin{aligned} \frac{\partial m}{\partial t} &= d(m - \dot{T}_H) \ , \\ \frac{\partial e}{\partial t} &= (e - \dot{T}_K) \ , \end{aligned} \tag{2.12}$$

with

$$\dot{T}_x = \frac{\partial \dot{g}}{\partial x} + 2m\frac{\partial \dot{H}}{\partial x} + e\frac{\partial \dot{K}}{\partial x}, \quad x = H, K \ . \tag{2.13}$$

In order to solve m and e from the coupled set of equations (2.12), we must provide appropriate boundary conditions. In Fig. 2 we have sketched the flow lines of the transformation (2.5). Due to the symmetry in H it suffices to consider only $H > 0$. Migdal's scheme, in its continuous form, works only in the ferromagnetic case $K > 0$. Note that $\dot{H} > 0$ and $\dot{K} < 0$ in this quadrant. Therefore H is always increasing and for K there is a competition between $(d-1)K$ and $\dot{K}$. For large H the function U becomes large for finite K and therefore any trajectory bends ultimately down to $K = 0$, except the axis $H = 0$, which exhibits a critical point at K_c satisfying

$$(d-1)K_c + \dot{K}(0, K_c) = 0 \ . \tag{2.14}$$

Using the simplification $H = 0$ in (2.8) we find for (2.14)

$$(d-1)K_c = -\tfrac{1}{2}\sinh 2K_c \ln \tanh K_c \ . \tag{2.15}$$

For $d = 2$ this implies the exact critical value $K_c = \frac{1}{2}\ln(\sqrt{2}+1)$ since Migdal's scheme preserves duality for $d = 2$.[4] For $K > K_c$ the coupling constant grows and for $K < K_c$ it decreases. Near $H = 0$ the trajectories follow this trend.

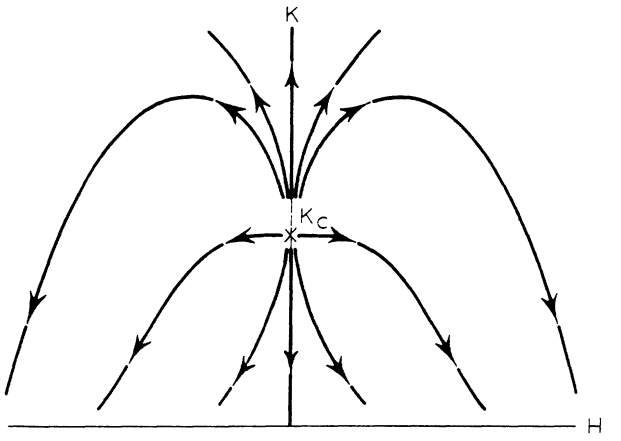

FIG. 2. Sketch of the flow lines of Migdal's transformation without shifting the magnetic fields.

Thus we must specify first of all the behavior of m and e in the small-K regime where the trajectories end. As this is a free system we have

$$m = \tanh H, \quad e = \tanh^2 H, \quad (K \to 0) \ . \tag{2.16}$$

We now inspect the flow equations in this regime and find

$$\begin{aligned} m - \dot{T}_H &= (m - \tanh H) + O(K \ln K) \ , \\ e - \dot{T}_K &= A \ln[(1 - \tanh^2 H)K] \\ &\quad + 2\tanh H(m - \tanh H) + O(K \ln K) \ , \end{aligned} \tag{2.17}$$

with

$$A = 2(m - \tanh H)\tanh H - (e - \tanh^2 H) \ . \tag{2.18}$$

One sees that to order $K \ln K$ the values (2.16) make the flow of m and e zero. Thus the boundary conditions (2.16) are compatible with the flow. It becomes insensitive to the time (or scale) on which the flow is reversed to calculate m, whenever the small-K region is reached.

It is also possible to impose directly a boundary condition at large H and arbitrary K for those trajectories that reach this zone. In this region the expressions for the flow simplify to

$$\begin{aligned} m - \dot{T}_H &= \frac{e-1}{2} + \frac{e^{-4K}}{2}(-1 + 2m - e) + O(e^{-2H}) \ , \\ e - \dot{T}_K &= e - 1 + \dot{K}_K(-1 + 2m - e) + O(e^{-2H}) \ , \end{aligned} \tag{2.19}$$

with

$$\dot{K}_K = e^{-4K}[-2H + 1 + \ln(1 - e^{-4K})] \ . \tag{2.20}$$

So we see that $m = e = 1$ [which matches with (2.16) for $H \to \infty$] remains invariant in the region H large, K finite. Once this regime is reached by the trajectory it makes no sense to continue the flow. Calculating the m and e upstream, it would yield a large stretch where the $m = e = 1$ values would be preserved.

Finally, we can impose a boundary condition at the

large-K, finite-H region. Here the flow simplifies to the expressions

$$m-\dot{T}_H=(1-e)\frac{\partial}{\partial H}\left[\frac{H}{2\tanh H}\right]+O(e^{-2K}),$$
$$e-\dot{T}_K=(e-1)+O(e^{-2K}). \tag{2.21}$$

Again the values $m=e=1$ are preserved in this regime. This explains also the spontaneous magnetization along the $H=0$ axis for $K>K_c$. For $H=0$ the expressions (2.7) reduce to

$$\dot{g}(0,K)=K+\cosh^2 K\ln(1+e^{-2K})-\sinh^2 K\ln(1-e^{-2K}),$$
$$\dot{H}(0,K)=0, \tag{2.22}$$
$$\dot{K}(0,K)=\tfrac{1}{2}\sinh 2K\ln\tanh K,$$

while we find for $\dot{T}_H$ for $H\to 0$,

$$m-\dot{T}_H=m\left[1-2\frac{\partial\dot{H}}{\partial H}\right]=m[1+\sinh 2K\ln(\tanh K)]. \tag{2.23}$$

In this limit $H\to 0$, m is no longer coupled to e. We then have to solve

$$\frac{\partial m}{\partial t}=dm[1+\sinh 2K\ln(\tanh K)] \tag{2.24}$$

in combination with the flow equation for K

$$\frac{\partial K}{\partial t}=(d-1)K+\tfrac{1}{2}\sinh 2K\ln\tanh K. \tag{2.25}$$

For $K\to\infty$ the flow of m stagnates, and in view of the previous considerations, we must put $m=1$ in the limit $H\to 0$. One may eliminate t from (2.24) and (2.25) in order to get a direct equation for m as function of K,

$$\frac{\partial m}{\partial K}=\frac{dm[1+\sinh 2K\ln(\tanh K)]}{(d-1)K+\frac{1}{2}\sinh 2K\ln\tanh K}, \tag{2.26}$$

which allows the solution

$$m_{\rm sp}(K)=\exp-\int_K^\infty dK'\frac{d[1+\sinh 2K'\ln(\tanh K')]}{(d-1)K'+\frac{1}{2}\sinh 2K'\ln(\tanh K')}, \tag{2.27}$$

in which the boundary condition $m_{\rm sp}(\infty)=1$ is built in. For $K\to K_c$ the integral diverges and $m_{\rm sp}$ vanishes as

$$m_{\rm sp}(K)\sim|K-K_c|^{(d-y_H)/y_T}=|K-K_c|^{\beta}, \tag{2.28}$$

as should be expected for the magnetization, with the exponents y_H and y_T given by

$$y_H=-d\sinh(2K_c)\ln(\tanh K_c)=2d(d-1)K_c,$$
$$y_T=d-2(d-1)K_c/\sinh 2K_c=d-y_H/(d\sinh 2K_c). \tag{2.29}$$

In Fig. 3 we have drawn the curve for the spontaneous magnetization as derived from (2.27) for $d=2$. Comparing it with the exact Onsager-Yang curve[6] one sees substantial deviations. These can be improved by shifting the fields together with the bonds for which one finds

$$m_{\rm sp}(K)=\exp-\int_K^\infty dK'\frac{1+\sinh 2K'\ln(\tanh K')}{(d-1)K'+\frac{1}{2}\sinh 2K'\ln(\tanh K')}, \tag{2.30}$$

which is also drawn in Fig. 3.

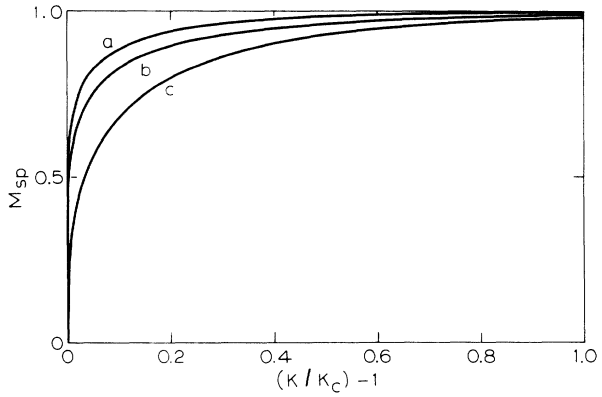

FIG. 3. Spontaneous magnetization ($d=2$) vs $(K/K_c)-1$ for (a) the exact Onsager-Yang solution, (b) Migdal's renormalization with shifting of the magnetic fields, and (c) without shifting the magnetic fields.

Solving the flow equations (2.12) and (2.13) as indicated above yields the (bulk) magnetization $m_b(H,K)$ as a function of H and K for the whole H,K plane. Most interesting is the behavior of $m_b(H,K)$ as a function of H for K near the critical value K_c. We have plotted in Fig. 4 three curves for $m_b(H)$: with K slightly larger than K_c, equal to K_c, and slightly below K_c. The figure shows how rapidly the curves change with K.

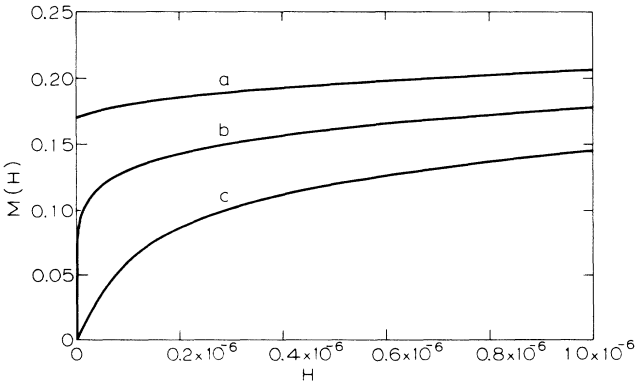

FIG. 4. Bulk magnetization $m_b(H,K)$ ($d=2$) as a function of the magnetic field H for (a) $K=1.001K_c$, (b) $K=K_c$, and (c) $K=0.999K_c$.

The magnetic equation of state $m_b(H,K)$ has a scaling behavior in the variables H and $\tau=K-K_c$ for small H and τ,

$$m_b(H,\tau)=\tau^{(d-y_H)/y_T}\overline{m}(H\tau^{-y_H/y_T}) . \tag{2.31}$$

Such a scaling behavior follows directly from the nature of the flow equations in the neighborhood of the critical point. For H and τ small, the flow equation (2.5) reduces to

$$\frac{\partial H}{\partial t}=y_H H ,$$
$$\frac{\partial \tau}{\partial t}=y_T \tau , \tag{2.32}$$

and the magnetization equation (2.12) becomes

$$\frac{\partial m}{\partial t}=(d-y_H)m , \tag{2.33}$$

where we have assumed that terms of order H may be omitted. We will show below that, indeed, $m \gg H$. The scaling form (2.31) satisfies (2.33) with the use of (2.32). The precise form of the scaling function $\overline{m}$ is not fixed by the form of (2.33) and (2.32) but must be obtained from the procedure outlined above.

The critical curve is the one in which m varies most rapidly with H as one sees in Fig. 4. Its shape can be deduced from (2.31) for $\tau \to 0$ and the requirement that the asymptotic behavior of $\overline{m}$ for large argument just compensates the power of τ in front of $\overline{m}$,

$$m_b(H,0) \sim H^{(d-y_H)/y_H}=H^{1/\delta} . \tag{2.34}$$

As δ is large one finds, indeed, $m \gg H$ as was assumed in (2.33).

III. INHOMOGENEOUS SYSTEMS

We consider now the case where the field H—and consequently the coupling constant K—depends on the position in the lattice and derive the appropriate flow formulas for the Hamiltonian and magnetization. It is assumed that continuous functions $H(z)$ and $K(z)$ exist depending on the longitudinal coordinate z. The earlier used notation H_n will be changed into $H(z_n)$ where z_n is the longitudinal position of site n. Bonds will be positioned based on the location of the middle of the bond. So transverse bonds have the same z as the sites which they connect while the longitudinal bonds have a z interpolating between the two sites.

The bond moving will be carried out in the same way as in the homogeneous case. This is less justified for the transverse bonds than for the longitudinal bonds. A longitudinal bond is moved (parallel to itself) to an equivalent position. A transverse bond is shifted, however, to a higher or a lower field area and extra errors are associated herewith. We note that always equal numbers are moved in opposite directions such that these extra errors tend to compensate. Moreover, bonds are moved preferably only when the field gradients are still small such that the inhomogeneity does not introduce substantial errors in the bond moving process.

As the longitudinal and transverse bonds behave differently in the renormalization process, we distinguish them by an index l and t. The shift of the longitudinal bonds is equal in all $d-1$ (transverse) directions leading to an effective bond $K_l^e(z)$ along the longitudinal edges

$$K_l^e(z)=b^{d-1}K_l(z) . \tag{3.1}$$

Along the transverse edges the effective coupling receives reenforcement from $d-2$ transverse directions and from the longitudinal direction. So we have

$$K_t^e(z)=b^{d-2}\sum_{j=-(b-1)/2}^{(b-1)/2} K_t(z+j) . \tag{3.2}$$

We will encounter frequently sums of this type. For sufficiently smooth functions $f(z)$ we may expand $f(z+j)$ around z and obtain

$$\sum_{j=-(b-1)/2}^{(b-1)/2} f(z+j)=bf(z)+\frac{1}{24}(b+1)b(b-1)\times\frac{\partial^2 f(z)}{\partial z^2}+\cdots . \tag{3.3}$$

The renormalized fields and couplings must now be calculated by eliminating the $(b-1)$ intermediate sites along the edges. For the transverse bonds this is almost identical to the homogeneous case because all the bonds and fields along the edges are of equal strength. The only difference is that the renormalized coupling is located at a new position $z'=z/b$ and that the effective coupling is calculated differently by (3.2) and (3.3). Writing for $b=1+dt$

$$K_t'(z/b)=K_t(z)+dt\left[\frac{\partial K_t}{\partial t}-z\frac{\partial K_t}{\partial z}\right] , \tag{3.4}$$

we find in the same way as in (2.5)

$$\frac{\partial K_t(z)}{\partial t}=z\frac{\partial K_t(z)}{\partial z}+(d-1)K_t(z)+\dot{K}(H(z),K(z))+\frac{1}{12}\frac{\partial^2 K_t(z)}{\partial z^2}+\cdots . \tag{3.5}$$

The first term on the right-hand side is a rescaling term originating from the renumbering of the sites in the renormalization process; the last term stems from the expansion (3.3).

For the longitudinal bonds we are faced with the decimation of $b-1$ intermediate sites along a chain in which the field (and also the coupling) varies. Although it is easy to carry out this decimation for arbitrary integer b, we have not been able to give the general formula for $b \to 1$. We limit ourselves to the case that the variations inside a cell are so small that we may replace bonds and fields by their value in the middle of the edge. Then the calculation of the renormalized longitudinal bond is the same as in the homogeneous case apart from the rescaling terms. So we find

$$\frac{\partial K_l(z)}{\partial t}=z\frac{\partial K_l(z)}{\partial z}+(d-1)K_l(z)+\dot{K}(H(z),K(z)) . \tag{3.6}$$

Such a flow equation misses terms of the type of the last term in (3.5). To be consistent we must omit it then also in (3.5) and restrict ourselves to inhomogeneities weak enough that second derivatives can safely be ignored. The distinction for the flow of the coupling constants between longitudinal and transverse then disappears and we work for both with the equation

$$\frac{\partial K(z)}{\partial t}=z\frac{\partial K(z)}{\partial z}+(d-1)K(z)+\dot{K}(H(z),K(z)) . \tag{3.7}$$

For the magnetic field we have $2(d-1)$ contributions from transverse directions and 2 from longitudinal directions. The latter are located at $z+(b/2)$ and $z-(b/2)$ when we consider a site at position z. So we have the flow equation for $b=1+dt$,

$$\begin{aligned}\frac{\partial H(z)}{\partial t}=&z\frac{\partial H(z)}{\partial z}+2(d-1)\dot{H}(H(z),K(z))\\&+\dot{H}(H(z-\tfrac{1}{2}),K(z-\tfrac{1}{2}))\\&+\dot{H}(H(z+\tfrac{1}{2}),K(z+\tfrac{1}{2})) .\end{aligned} \tag{3.8}$$

To be consistent with (3.7) we must ignore the fact that in the longitudinal contributions the fields are not at the same value of z as in the transverse terms. Expanding these terms around the point z, only contributions of second order in the gradients or second-order derivatives survive; the linear terms cancel. As second-order derivatives are left out in (3.7), we reduce (3.8) also to

$$\frac{\partial H(z)}{\partial t}=z\frac{\partial H(z)}{\partial z}+2d\dot{H}(H(z),K(z)) . \tag{3.9}$$

The flow equations (3.7) and (3.9) are reliable as long as the variation of $H(z)$ and $K(z)$ with z is weak.

The derivation of the flow equation for the magnetization $m(z)$ is more delicate because we must be prepared that the variation of $m(z)$ with z is stronger than that of $H(z)$. Another difference is that one obtains, in general, different equations for different positions in the cell shown in Fig. 1. For example, the field on the corners enters in a different way in the renormalized field H' than the fields on the edges or in the center of the cell. To approach this problem carefully we rewrite the general equations (1.6) and (1.8) using the continuous functions $H(z)$ and $K(z)$. As in the transition to the homogeneous case we sum the equations now over the $d-1$ transverse directions. This leads to

$$\begin{aligned}b^{d-1}m(z)=&\frac{\delta\tilde{g}}{\delta H(z)}+\sum_{z'}\left[m'(z')\frac{\delta H'(z')}{\delta H(z)}\right.\\&+(d-1)e_t'(z')\frac{\delta K_t'(z')}{\delta H(z)}\\&\left.+e_l'(z')\frac{\delta K_l'(z')}{\delta H(z)}\right],\\b^{d-1}e_t(z)=&\frac{\delta\tilde{g}}{\delta K_t(z)}+\sum_{z'}\left[m'(z')\frac{\delta H'(z')}{\delta K_t(z)}\right.\\&\left.+e_t'(z')\frac{\delta K_t'(z')}{\delta K_t(z)}\right],\\b^{d-1}e_l(z)=&\frac{\delta\tilde{g}}{\delta K_l(z)}+\sum_{z'}\left[m'(z')\frac{\delta H'(z')}{\delta K_l(z)}\right.\\&\left.+e_l'(z')\frac{\delta K_l'(z')}{\delta K_l(z)}\right],\end{aligned} \tag{3.10}$$

where $\tilde{g}=(N')^{-(d-1)/d}G$ and the variation with respect to $K_t(z)$ refers to one of the transverse orientations. Possible cross terms between the transverse e_t and longitudinal e_l are absent because the flows of longitudinal and transverse bonds are uncoupled.

In (3.10) it matters whether z is taken at a corner site or at intermediate points. In order to make the $b\to 1$ limit we calculate averages over these equations and apply (3.3)

$$\begin{aligned}&\sum_{j=-(b-1)/2}^{(b-1)/2}b^{d-1}m(z+j)\\&\quad=b^d\left[m(z)+\frac{1}{24}(b+1)(b-1)\frac{\partial^2 m(z)}{\partial z^2}+\cdots\right].\end{aligned} \tag{3.11}$$

For $m(z)$ and $e_t(z)$ we make such averages by taking z at a corner of a cell and for $e_l(z)$ we take z in the middle of a longitudinal chain. The derivation of the flow equation for the transverse $e_t(z)$ is the simplest, as the terms in the average (3.11) refer to derivatives with respect to exactly the same $K_t(z+j)$, which build, according to (3.2), the effective transverse bond $K_t^e(z)$. So all the terms in the average contribute an equal amount since $H'(z')$ and $K_t'(z')$ depend only on $K_t^e(z)$ with $z'=z/b$. Putting these points together we have

$$\begin{aligned}&b^d\left[e_t(z)+\frac{(b+1)(b-1)}{24}\frac{\partial^2 e_t(z)}{\partial z^2}+\cdots\right]\\&\quad=b^{d-1}\left[\frac{\delta\tilde{g}}{\delta K_t^e(z)}+m'\left[\frac{z}{b}\right]\frac{\delta H'(z/b)}{\delta K_t^e(z)}\right.\\&\qquad\left.+e_t'\left[\frac{z}{b}\right]\frac{\delta K'(z/b)}{\delta K_t^e(z)}\right] .\end{aligned} \tag{3.12}$$

As before, we set in the limit $b\to 1$

$$e_t'(z/b)=e_t(z)+\left[-z\frac{\partial e_t(z)}{\partial z}+\frac{\partial e_t(z)}{\partial t}\right]dt , \tag{3.13}$$

and use the expressions (2.3). Then we obtain for $b \to 1$

$$\frac{\partial e_t(z)}{\partial t} = z\frac{\partial e_t(z)}{\partial z} + e_t(z) - \dot{T}_k(z) + \left[\frac{1}{12}\frac{\partial^2 e_t(z)}{\partial z^2} + \cdots\right] . \quad (3.14)$$

$\dot{T}_k(z)$ has the same definition as in (2.13) but now evaluated with the fields $H(z)$ and $K(z)$ and with $m(z)$ and $e_t(z)$ substituted for m and e.

The equation for the longitudinal $e_l(z)$ follows from (3.10) by averaging over all the bonds along a longitudinal chain [see Fig. 5(a)]. As before we approximate the evaluation of the derivatives inside the chain as if there is no variation with position, i.e., we evaluate them at the value z in the middle of the chain. Then we obtain in analogy with (3.14)

$$\frac{\partial e_l(z)}{\partial t} = z\frac{\partial e_l(z)}{\partial z} + e_l(z) - \dot{L}_k(z) + \left[\frac{1}{12}\frac{\partial^2 e_l(z)}{\partial z^2} + \cdots\right] , \quad (3.15)$$

with $\dot{L}_K(z)$ defined as

$$\dot{L}_K(z) = \frac{\partial \dot{g}}{\partial K}(z) + [m(z-\tfrac{1}{2}) + m(z+\tfrac{1}{2})]\frac{\partial \dot{H}}{\partial K}(z) + e_l(z)\frac{\partial \dot{K}}{\partial K}(z) . \quad (3.16)$$

In contrast to $\dot{T}_K(z)$, $\dot{L}_K(z)$ couples to $m(z-\frac{1}{2})$ and $m(z+\frac{1}{2})$ at the ends of the longitudinal bond.

The equation for $m(z)$ has a mix of these transverse and longitudinal ingredients. The transverse contributions are straightforward, as all happens at the same z. For the longitudinal contributions we have the complication that half of the average is over the left chain and the other half over the right chain [see Fig. 5(b)]. We show in Appendix B that in the limit of vanishing gradients of the field, the sum of the derivatives with respect to the fields of the left half or right half gives equally one-half of the total derivative. Consequently, we arrive at

$$\frac{\partial m(z)}{\partial t} = z\frac{\partial m(z)}{\partial z} + dm(z) - [(d-1)\dot{T}_H(z) + \tfrac{1}{2}\dot{L}_H(z-\tfrac{1}{2}) + \tfrac{1}{2}\dot{L}_H(z+\tfrac{1}{2})] + \left[\frac{1}{12}\frac{\partial^2 m}{\partial z^2} + \cdots\right] . \quad (3.17)$$

We see from (3.16) and (3.17) that these flow equations are nonlocal. In particular, $m(z)$ and $e_l(z)$ are coupled to the values at shifted positions. By writing in (3.16)

$$m(z-\tfrac{1}{2}) + m(z+\tfrac{1}{2}) = 2m(z) + \frac{1}{4}\frac{\partial^2 m(z)}{\partial z^2} + \cdots , \quad (3.18)$$

we may replace $\dot{L}_K(z)$ by

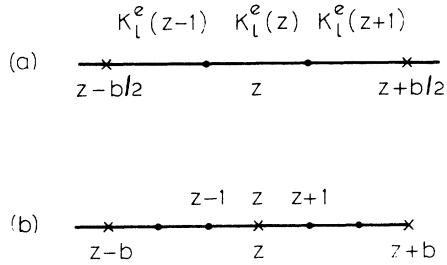

FIG. 5. Illustrative chain segments used in the averaging of (a) $e_l(z)$ and (b) $m(z)$. Crosses correspond to corner sites.

$$\dot{L}_K(z) = \dot{T}_K(z) + \frac{1}{4}\frac{\partial \dot{H}}{\partial K}(z)\frac{\partial^2 m(z)}{\partial z^2} + \cdots , \quad (3.19)$$

and insert this into (3.15) yielding

$$\frac{\partial e_l(z)}{\partial t} = z\frac{\partial e_l(z)}{\partial z} + e_l(z) - \dot{T}_K(z) + \left[\frac{1}{12}\frac{\partial^2 e_l(z)}{\partial z^2} - \frac{1}{4}\frac{\partial \dot{H}}{\partial K}(z)\frac{\partial^2 m(z)}{\partial z^2}\right] + \cdots . \quad (3.20)$$

This makes the longitudinal flow equation for $e_l(z)$ nearly the same as the transverse equation (3.14). The last term in (3.20) is of minor importance, being odd in the magnetic field and thus vanishing for small fields. We will simplify the flow equations for $e_l(z)$ and $e_t(z)$ even further by omitting all nonlocal terms. As a first approximation this is justified because $e_l(z)$ and $e_t(z)$ become very smooth functions of z across the interface. In both phases e_l and e_t have the same value and all variation is induced by the variation of $m(z)$, which has opposite values in the two phases. Thus we replace (3.14) and (3.20) by one equation

$$\frac{\partial e(z)}{\partial t} = z\frac{\partial e(z)}{\partial z} + e(z) - \dot{T}_K(z) . \quad (3.21)$$

In the same spirit we simplify (3.17) by ignoring all nonlocality except for the variations of $m(z)$. Then (3.17) can be written as

$$\frac{\partial m(z)}{\partial t} = z\frac{\partial m(z)}{\partial z} + d[m(z) - \dot{T}_H(z)] + \left[\frac{\partial m}{\partial t}\right]_{\text{nonloc}} , \quad (3.22)$$

with the nonlocal term

$$\left[\frac{\partial m}{\partial t}\right]_{\text{nonloc}} = \left[\frac{1}{12} - \frac{1}{2}\frac{\partial \dot{H}}{\partial H}(z)\right]\frac{\partial^2 m}{\partial z^2} . \quad (3.23)$$

In contrast to $\partial \dot{H}/\partial K$, the derivative $\partial \dot{H}/\partial H$ is even in the field and has a finite value for $H \to 0$.

The equations (3.21) and (3.22) from the basis for our calculations. They need the solution of the flow (3.7) and (3.9) for $K(z)$ and $H(z)$ as an input. In (3.21) and (3.22)

all nonlocal effects are omitted except those associated with the spatial variation of $m(z)$, which is the characteristic of an interface. Since the nonlocal term (3.23) is expressed in the second derivative of $m(z)$ (leaving out higher derivatives), the validity is restricted to smoothly varying $m(z)$.

IV. SOLUTION OF THE FLOW EQUATIONS

The analysis of the flow equations (3.21) and (3.22) proceeds by a transformation which eliminates the spatial rescaling term. We define $\hat{m}$

$$m(z,t)=\hat{m}(Aze^{t},t) , \tag{4.1}$$

and similarly $\hat{K}$, $\hat{H}$, and $\hat{e}$. Inserting these definitions into (3.22) yields

$$\frac{\partial\hat{m}(v,t)}{\partial t}=d[\hat{m}(v,t)-\dot{T}_H(v,t)] + A^2e^{2t}\left[\frac{1}{12}-\frac{1}{2}\frac{\partial\dot{H}}{\partial H}\right]\frac{\partial^2\hat{m}(v,t)}{\partial v^2} . \tag{4.2}$$

In all the other equations (3.7), (3.9) and (3.21) only the rescaling term drops and for any v

$$v=Aze^{t} , \tag{4.3}$$

these equations are the same as the local equations (2.5) and (2.12).

The amplitude A is introduced for calculational convenience. It must reduce the increasing exponential e^{2t} in front of the nonlocal term in (4.2). For definiteness we write out $\dot{T}_H$ as given by (2.13)

$$\dot{T}_H(v,t)=\frac{\partial\dot{g}}{\partial H}+2\hat{m}(v,t)\frac{\partial\dot{H}}{\partial H}+\hat{e}(v,t)\frac{\partial\dot{K}}{\partial H} , \tag{4.4}$$

where the derivatives $\partial\dot{g}/\partial H$, etc., are evaluated at the field $\hat{H}(v,t)$ and coupling constant $\hat{K}(v,t)$.

If we were to ignore the nonlocal term in (4.2) we would obtain the local solution for $m(z,t)$. It would result as follows. Starting from the initial field distribution given by (1.2)

$$\hat{H}(v,0)=H(v/A,0)=gv/A , \quad \hat{K}(v,0)=K(v/A,0)=K , \tag{4.5}$$

the values $\hat{H}(v,t_f)$ and $\hat{K}(v,t_f)$ are computed for sufficiently large t_f with v as a fixed parameter. At t_f the boundary conditions for $\hat{m}(v,t_f)$ and $\hat{e}(v,t_f)$ are imposed as indicated in Sec. II. With the (local) equations for $\hat{m}(v,t)$ and $\hat{e}(v,t)$ the values at $t=0$ are computed and

$$m(z,0)=\hat{m}(Az,0) \tag{4.6}$$

yields the desired magnetization. The whole operation amounts to the insertion of the form (1.2) into the bulk equation of state $m_b(H,K)$

$$m(z,0)=m_b(gz,K) . \tag{4.7}$$

This sets the scenario for the influence of the nonlocal term in (4.2), which we will call the diffusion term because of its role analogous to the diffusion process. We distinguish the cases where $K \gtrless K_c$ initially.

A. High-temperature regime $K < K_c$

For $K < K_c$ the initial values (4.5) are mapped onto the line $K=0$. The point $v=0$ (or $\hat{H}=0$) is the slowest in approaching $\hat{H}=0$, $\hat{K}=0$ as is indicated in Fig. 6. During the renormalization process the gradient in $\hat{H}(v,t)$ with respect to v increases, but for sufficiently low initial g the gradient can be kept small such that $\hat{H}(v,t)$ remains smooth when the small-K regime is reached. Then the boundary condition (2.16) applies,

$$\hat{m}(v,t_f)=\tanh[\hat{H}(v,t_f)] , \quad \hat{e}(v,t_f)=\tanh^2[\hat{H}(v,t_f)] . \tag{4.8}$$

Flowing back, the solution of (4.2) will follow the local solution since the diffusion term can be made arbitrarily small by letting $g\to 0$. From (4.7) one sees that the second derivative is of order g^2. When K approaches K_c a conflict arises, however, because the point $v=0$ on the $H=0$ axis takes longer and longer to reach $K=0$.

B. Critical case $K=K_c$

For $K=K_c$ the initial values start to spread along the flow line which starts horizontally in the fixed point $H=0$, $K=K_c$ and along the fixed line $K=0$ (see Fig. 6). We will call this flow line the critical flow line. It meets the line $K=0$ at a relatively high value of H ($\simeq 3$ for $d=2$). Thus the points for finite v, ending at $K=0$, have practically $\hat{m}=\hat{e}=1$ as boundary values. The part along the critical flow line has to provide the smooth transition to $\hat{m}=0$ for $v=0$ (or $\hat{H}=0$). In the small-K regime the variation of $\hat{H}$ with v along the critical flow line is rapid no matter how small the initial g is. Thus we run out of the validity regime of the flow equations for which smooth variation with respect to the spatial variation is assumed. In practice we have handled this difficulty as

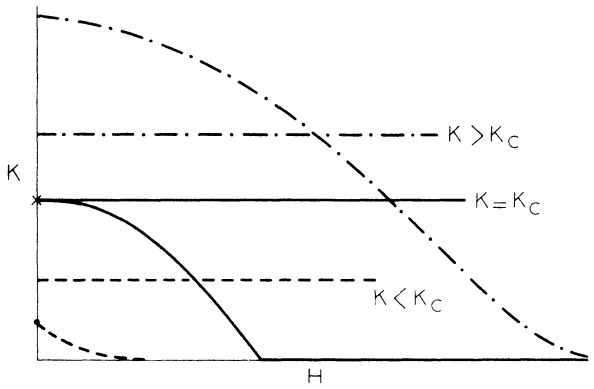

FIG. 6. K and H values at the start (horizontal lines) and corresponding values at the end (curved lines) of the renormalization.

follows. We solve the differential equations by taking a discrete set of points $v=0,1,\ldots$ (the distances in v are irrelevant because the gradient g can be varied and only gv matters). The flow of $\hat{H}$ and $\hat{K}$ is carried out until for $v=1$ a sufficiently small $\hat{K}$ is reached. Then the boundary conditions (4.8) are imposed and $\hat{m}$ and $\hat{e}$ are flowed back to $t=0$. This flow backwards works only when A is well chosen. For $A=1$ any noise in $\hat{m}$ is amplified immediately in the diffusion term due to the large exponential in front of it. For $A=e^{-t_f}$ the diffusion term behaves well, but the important information for $m(z,0)$ in (4.6) is hidden in the small-v behavior of $\hat{m}(v,0)$ for which no points exist. Values of the order $A=10e^{-t_f}$ lead to stable results insensitive to A and t_f for a wide range of A and t_f. This works for values of K close to K_c.

For small $\tau=K-K_c$ the magnetization obeys the scaling law

$$m(z;g,\tau)=g^{(d-y_H)/(y_H+1)} \times \tilde{m}(zg^{1/(y_H+1)},\tau g^{-y_T/(y_H+1)}) , \tag{4.9}$$

with y_H and y_T given by (2.29). Such a scaling law follows from the observation that the diffusion term works only in the final stages of the renormalization process and most of the time the local equations apply.

Thus the local equations are of the form (2.30) and (2.25), which we translate to

$$\frac{\partial g}{\partial t}=g(y_H+1), \quad \frac{\partial \tau}{\partial t}=y_T\tau . \tag{4.10}$$

The local equation for m reads as (2.31)

$$\frac{\partial m(z,t)}{\partial t}=z\frac{\partial m(z,t)}{\partial z}+(d-y_H)m(z,t) , \tag{4.11}$$

and one sees that (4.9) obeys (4.11) for any $\tilde{m}$. The precise form of $\tilde{m}$ follows from the boundary condition and from the final stages of the renormalization flow where the diffusion term is active.

In Fig. 7 we have plotted the critical curve ($\tau=0$) together with one for $\bar{\tau}=\tau g^{-y_T/(y_H+1)}=1$ and one for $\bar{\tau}=-0.3$ for $d=2$.

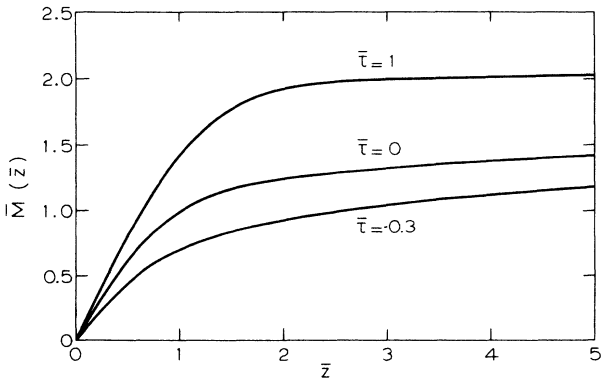

FIG. 7. Scaled magnetization $\bar{m}=g^{(y_H-d)/(y_H+1)}m$ vs $\bar{z}=g^{1/(y_H+1)}z$ for three scaling parameters $\bar{\tau}=\tau g^{-y_T/(y_H+1)}$ and $d=2$.

C. Low-temperature regime $K>K_c$

As indicated in Fig. 6 the initial data (4.5) for $K>K_c$ develop after some time in a curve which runs from small H and large K to small K and large H. In the local approximation one would use for all values $\hat{m}=\hat{e}=1$. This leads to a discontinuity for $H=0$ since $\hat{m}=-1$ for $H<0$. As our flow equations are inaccurate for discontinuous $\hat{m}(v,t)$ we must see which boundary conditions are compatible with the flow. Fortunately the flow simplifies considerably in the regime of large K. With (2.21) and $\hat{e}=1$, we find that (4.2) reduces to

$$\frac{\partial \hat{m}(v,t)}{\partial t}=-\frac{A^2e^{2t}}{6}\frac{\partial^2\hat{m}(v,t)}{\partial v^2} , \tag{4.12}$$

which has the solution

$$\hat{m}(v,t)=\int_{-\infty}^{\infty}dv'\frac{e^{-(v-v')^2/4Q(t)}}{\sqrt{4\pi Q(t)}}\hat{m}(v',t_f) , \tag{4.13}$$

with

$$Q(t)=\tfrac{1}{12}A^2(e^{2t_f}-e^{2t}) . \tag{4.14}$$

Equation (4.13) tells us how $\hat{m}(v,t)$ behaves when $\hat{m}(v,t_f)$ is given for some distant time t_f. When t_f and t are far apart, the value of $Q(t)$ becomes independent of t and thus $\hat{m}(v,t)$ approaches a fixed distribution, involving the still arbitrary constant

$$Q=\tfrac{1}{12}A^2e^{2t_f} . \tag{4.15}$$

We can turn this around and say that A equals

$$A=\sqrt{12Q}\,e^{-t_f} . \tag{4.16}$$

We can safely assume that the interface profile $m(z,t_f)$ is sharp when K is large and the gradient in $H(z,t)$ of order unity. For large t the gradient grows as

$$g(t)=e^{(d+1)t}g \tag{4.17}$$

since $\partial\dot{H}/\partial H\simeq\frac{1}{2}$ for large K. So we estimate that

$$e^{-t_f}\simeq g^{1/(d+1)} . \tag{4.18}$$

Now combining (4.6), (4.16), and (4.18) we find

$$m(z,0)=\hat{m}(\sqrt{12Q}\,zg^{1/(d+1)},0) . \tag{4.19}$$

This expression shows that $m(z,0)$ is a function of the combination $zg^{1/(d+1)}$, which means that the interface profile is rough; it spreads over a wider and wider region when $g\to 0$. The effective width of the interface behaves as

$$w\sim g^{-1/(d+1)} , \tag{4.20}$$

which has to be compared with the capillary-wave theory yielding

$$w\sim g^{-(3-d)/4} . \tag{4.21}$$

For $d\simeq 1$ the two formulas agree to order $d-1$

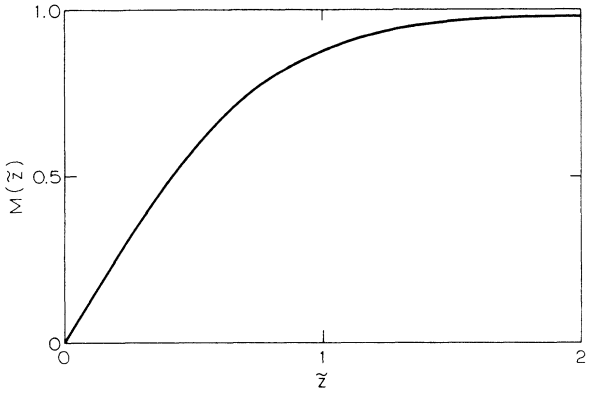

FIG. 8. Magnetization m vs $\tilde{z}=g^{1/(d+1)}z$ for $K=2K_c$ and $d=2$.

$$\frac{1}{d+1}=\frac{1}{2}-\frac{d-1}{4}+\cdots, \quad \frac{3-d}{4}=\frac{1}{2}-\frac{d-1}{4} . \tag{4.22}$$

Apart from this qualitative behavior we have still to fix Q. We do this by considering the $d=1$ theory where the exact profile is known.[7] For $d=1$ the Migdal procedure is exact, but the flow equation (4.2) is still an approximation. The exact solution is recovered from (4.13) for

$$\hat{m}(v,t_f)=\mathrm{sgn}v \tag{4.23}$$

and

$$Q=\tfrac{1}{4} . \tag{4.24}$$

So we adapt this choice (4.23) and (4.24) as a proper combination for the description of the low-temperature interfaces.

In Fig. 8 we have plotted a low-temperature interface in $d=2$ and $K=2K_c$ as it is calculated from (4.2) and (4.23) with the choice (4.16) and (4.24) for A.

V. DISCUSSION

Using Migdal's renormalization procedure interfacial profiles are calculated for nearly critical and for low-temperature conditions. The profiles are obtained from an extension of the calculation of the equation of state, i.e., as the magnetization for a system in which the magnetic field varies linearly in space. The gradient g of the magnetic field is taken arbitrarily small and as a result the interface is also slowly varying in space, but generally not on the same scale as the field.

Above the critical temperature the resulting magnetization profile is the bulk magnetization following locally the varying field. Thus the scale on which the "interface" varies is g^{-1} just as that of the field [see (4.7)].

The nearly critical interface varies on a scale $g^{-1/(y_H+1)}$ where y_H is the magnetic critical exponent. The interface has a scaling form (4.9) which interpolates between the high- and low-temperature behavior.

Below T_c we find an interface of a width $g^{-1/(d+1)}$ [see (4.20)] which resembles the smearing out of the interface due to capillary waves. We comment on the discrepancy with the capillary scale $g^{-(3-d)/4}$ further below.

For the interesting cases the interface varies more rapidly in space than the field that induces the interface. We have taken advantage of the slow variation of the field by ignoring the nonlocal effects in the flow of the field. Nonlocal effects are, however, essential in the interface formation near and below the critical point.

In this calculation we have used the continuous rescaling formulation of the Migdal bond shifting technique. The main reason is that for an integer rescaling ($b=2,3,\ldots$) Migdal's renormalization leads to irregularities in the interface due to the fact that a distinction is made between sites which are removed and those which are kept. For example, for $b=2$ a difference between even and odd sites is introduced, which is an artifact of the shifting procedure since it disappears for $d=1$. One can smooth out this noise by more refined shifting techniques, but we feel that such a sophistication does not lead to a more convincing theory. For $b\to 1$ the equivalence between the sites is restored in a natural way.

The continuous Migdal procedure has the drawback that it cannot be implemented when the field gradient starts to be of order unity. This presents a problem at the end of the renormalization process where larger field gradients appear. As the order parameter varies faster than the field, the final stages of the renormalization are clear.

When the field varies of order unity the interface is practically sharp. Qualitative features as the width of the interfaces are insensitive to the details at the boundary. The quantitative form does depend on the precise moment when the field gradient is considered strong enough to impose a step function as interface. Even in $d=1$, where Migdal is exact, this ambiguity remains for a continuous Migdal transformation. For $d=1$ we do know,[7] however, the precise interface and from the $d=1$ behavior we have deduced the criterion (4.24) to fix the interface in all dimensions d.

The above-mentioned difficulties with discrete and continuous Migdal transformations may be considered as technical in the sense that they will disappear when a more sophisticated renormalization procedure is taken. More serious is the discrepancy between the low-temperature behavior (4.20) found in this paper and the capillary-wave behavior (4.21). As the bond shifting is the only uncontrollable error, one could again blame it for this mismatch. However, the exponent of the low-temperature width of the interface is directly related to the fact that the magnetic exponent equals the dimensionality $y_H=d$ for $T=0$. This property of the discontinuity fixed point will not be changed in a better transformation.

The source of the discrepancy must be located in the character of the nonlocal term (3.23) in the flow equation for the magnetization. This diffusion term overestimates the effect of the nonlocality in the flow. The amplitude of the diffusion must vanish in a certain way for $T\to 0$ instead of approaching a constant value as it does now. Then a sharp profile is maintained longer on the way back from the high gradient regime, leading to a narrower width for the interface than found in this paper.

Then also the special role of $d=3$ should become clear and the roughening transition for $d=3$ should emerge.[8] This is the object of further study.

ACKNOWLEDGMENTS

One of the authors (J.M.J.v.L.) gratefully acknowledges the hospitality of the Physics Department of the Saint Francis Xavier University in Antigonish, Nova Scotia, Canada, where part of this work was done. G.L.M.D. acknowledges support from CNPq-Brazilian Agency for Scientific and Technological Development. Part of this research was supported by the Stichting voor Fundamenteel Onderzoek der Materie (FOM), which is financially supported by the Nederlandse Organisatie voor Wetenschappelijk Onderzoek (ZWO).

APPENDIX A

The basic one-dimensional reduction relation is given by the formula (2.2), which can be written in the transfer matrix form with the aid of a matrix

$$R_{ss'}=\exp(K_e ss'+\tfrac{1}{2}H(s+s')) \tag{A1}$$

as

$$\exp[g+K'ss'+(H_d+\tfrac{1}{2}H)(s+s')]=(R^b)_{ss'}\ , \tag{A2}$$

where R^b is the b power of the matrix R. The eigenvalues of R are given by

$$\lambda_{\pm}=e^{K_e}\cosh H[1\pm q(H,K_e)]$$

with

$$q(H,K_e)=[\tanh^2 H+e^{-4K}(1-\tanh^2 H)]^{1/2}\ . \tag{A3}$$

R is diagonalized by a matrix B

$$D_{ss'}=(B^T R B)_{ss'}=\lambda_s\delta_{ss'}\ , \tag{A4}$$

which is explicitly given by

$$B_{ss'}=(1+r^2)^{-1/2}[r\delta_{ss'}+s'(s-\delta_{ss'})]\ . \tag{A5}$$

B^T is the transposed matrix and r equals

$$r=e^{2K_e}\sinh H\left[1+\left[1+\frac{e^{-4K_e}}{\sinh^2 H}\right]^{1/2}\right]\ . \tag{A6}$$

So we find for $(R^b)_{ss'}$

$$(R^b)_{ss'}=(BD^bB^T)_{ss'}=\sum_{s''}B_{ss''}\lambda_{s''}^b B^T_{s''s'}\ . \tag{A7}$$

Now we may take the limit $b=1+dt$.

Expanding the decimation equation (A2) in dt using (A7), (2.3), and

$$\lambda_{s''}^b=\lambda_{s''}(1+dt\,\ln\lambda_{s''})\ , \tag{A8}$$

we get to zeroth order (for possible values of s and s')

$$\begin{aligned} e^{H+K_e}&=(r^2\lambda_+ +\lambda_-)/(1+r^2)\ ,\\ e^{-K_e}&=r(\lambda_+-\lambda_-)/(1+r^2)\ ,\\ e^{-H+K_e}&=(\lambda_+ +r^2\lambda_-)/(1+r^2)\ , \end{aligned} \tag{A9}$$

and to first order, using the zeroth-order result,

$$\begin{aligned} \dot g+\dot K+2\dot H&=\frac{r^2\lambda_+\ln\lambda_+ +\lambda_-\ln\lambda_-}{r^2\lambda_+ +\lambda_-}\ ,\\ \dot g-\dot K&=\frac{\lambda_+\ln\lambda_+ -\lambda_-\ln\lambda_-}{\lambda_+-\lambda_-}\ ,\\ \dot g+\dot K-2\dot H&=\frac{\lambda_+\ln\lambda_+ +r^2\lambda_-\ln\lambda_-}{\lambda_+ +r^2\lambda_-}\ , \end{aligned} \tag{A10}$$

from which $\dot g$, $\dot K$, and $\dot H$ can be solved. Inserting the expressions for $\lambda_\pm$ and r and some straightforward algebra lead to Eqs. (2.7).

APPENDIX B

We want to show that

$$\sum_{j=1}^{(b-1)/2}\frac{\delta}{\delta H(z+j)}=\frac{1}{2}\sum_{j=1}^{b-1}\frac{\delta}{\delta H(z+j)} \tag{B1}$$

in the limit $b\to 1$. Shifting the bonds leads to effective coupling constants $K_l^e(z)=b^{d-1}K_l(z)$.

Decimation of the resulting one-dimensional chain defines g, K_l', H^r, and H^l by

$$\begin{aligned} \sum_{s_1\cdots s_{b-1}=\pm1}&\exp[K_l^e(z+\tfrac{1}{2})ss_1+\cdots+K_l^e(z+b-\tfrac{1}{2})s_{b-1}s'+H(z+1)s_1+\cdots+H(z+b-1)s_{b-1}]\\ &\equiv\exp[g(z'+\tfrac{1}{2})+K_l'(z'+\tfrac{1}{2})ss'+H^r(z')s+H^l(z'+1)s']\ . \end{aligned} \tag{B2}$$

Variation of the field $H(z+j)$ gives

$$\frac{\delta g(z'+\frac{1}{2})}{\delta H(z+j)}+\frac{\delta K_l'(z'+\frac{1}{2})}{\delta H(z+j)}ss'+\frac{\delta H^r(z')}{\delta H(z+j)}s+\frac{\delta H^l(z'+1)}{\delta H(z+j)}s'=\langle s_j\rangle_{ss'}\ , \tag{B3}$$

with

$$\langle s_j\rangle_{ss'}\equiv\frac{\sum_{s_1\cdots s_{b-1}=\pm1}s_j\exp[K_l^e(z+\frac{1}{2})ss_1+\cdots+K_l^e(z+b-\frac{1}{2})s_{b-1}s'+H(z+1)s_1+\cdots+H(z+b-1)s_{b-1}]}{\sum_{s_1\cdots s_{b-1}=\pm1}\exp[K_l^e(z+\frac{1}{2})ss_1+\cdots+K_l^e(z+b-\frac{1}{2})s_{b-1}s'+H(z+1)s_1+\cdots+H(z+b-1)s_{b-1}]}\ , \tag{B4}$$

and therefore

$$\frac{\delta g(z'+\frac{1}{2})}{\delta H(z+j)}=\frac{1}{4}\sum_{ss'}\langle s_j\rangle_{ss'},\quad \frac{\delta K_l'(z'+\frac{1}{2})}{\delta H(z+j)}=\frac{1}{4}\sum_{ss'}ss'\langle s_j\rangle_{ss'},$$
$$\frac{\delta H^r(z')}{\delta H(z+j)}=\frac{1}{4}\sum_{ss'}s\langle s_j\rangle_{ss'},\quad \frac{\delta H^l(z'+1)}{\delta H(z+j)}=\frac{1}{4}\sum_{ss'}s'\langle s_j\rangle_{ss'}. \tag{B5}$$

Replacing all coupling constants and fields by the K_l, H at the middle of the edge and introducing the transfer matrix

$$R_{s_i s_{i+1}}=\exp[K_l s_i s_{i+1}+\tfrac{1}{2}H(s_i+s_{i+1})]$$

allows us to write

$$\langle s_j\rangle_{ss'}=\frac{R_{ss_1}\cdots R_{s_{j-1}s_j}s_j R_{s_j s_{j+1}}\cdots R_{s_{b-1}s'}}{R_{ss_1}\cdots R_{s_{b-1}s'}}. \tag{B6}$$

A suitable basis transformation B will diagonalize R: $R=BDB^T$ with $D_{ss'}=\Lambda_s\delta_{ss'}$. This makes

$$\langle s_j\rangle_{ss'}=\frac{\sum_{r,t,s_j=\pm1}B_{sr}\Lambda_r^j B^T_{rs_j}s_j B_{s_j t}\Lambda_t^{b-j}B^T_{ts'}}{\sum_{r=\pm1}B_{sr}\Lambda_r^b B^T_{rs'}}. \tag{B7}$$

Summation of the equations in (B5) over j leads ultimately to the summation

$$\begin{aligned}\sum_{j=1}^{n}\Lambda_r^j\Lambda_t^{b-j}&=\Lambda_r^b\left[n\delta_{rt}+(1-\delta_{rt})\sum_{j=1}^{n}\left[\frac{\Lambda_r}{\Lambda_t}\right]^j\right],\quad n=b-1 \text{ or } (b-1)/2\\&=\Lambda_r^b\left[n\delta_{rt}+(1-\delta_{rt})\frac{\Lambda_r}{\Lambda_t}\left[\frac{1-(\Lambda_r/\Lambda_t)^n}{1-\Lambda_r/\Lambda_t}\right]\right],\\&=n\Lambda_r^b\left[\delta_{rt}+(1-\delta_{rt})\frac{\ln(\Lambda_r/\Lambda_t)}{(1-\Lambda_t/\Lambda_r)}\right],\quad \text{in the limit } b\to1.\end{aligned} \tag{B8}$$

This last equation holds only in the limit $b\to1$ since

$$\left[\frac{\Lambda_r}{\Lambda_t}\right]^n=\exp\left[n\ln\left[\frac{\Lambda_r}{\Lambda_t}\right]\right]\simeq1+n\ln\left[\frac{\Lambda_r}{\Lambda_t}\right],\quad \text{when } n\to0\ (b\to1). \tag{B9}$$

Thus the summation is proportional to n and therefore (B1) holds.

---

*Permanent address: Departamento de Física-CCI, Universidade Federal da Paraiba (UFPb)-Campus II 58100, Campina Grande (Pb), Brazil.

[1]J. D. van der Waals, Ph.D. thesis, University of Leiden, 1873; J. S. Rowlinson, J. Stat. Phys. **20**, 197 (1979).

[2]F. P. Buff, R. A. Lovett, and F. H. Stillinger, Phys. Rev. Lett. **15**, 621 (1965).

[3]J. M. J. van Leeuwen and J. V. Sengers, Physica A **138**, 1 (1986).

[4]A. A. Migdal, Zh. Eksp. Teor. Fiz. **69**, 810 (1975); **69**, 1457 (1975) [Sov. Phys.—JETP **42**, 413 (1976); **42**, 743 (1976)]; T. W. Burkhardt, in *Real-Space Renormalization,* Vol. 30 of *Topics in Current Physics,* edited by T. W. Burkhardt and J. M. J. van Leeuwen (Springer-Verlag, Berlin, 1982), p. 33.

[5]M. J. Oliveira, D. Furman, and R. B. Griffiths, Phys. Rev. Lett. **40**, 977 (1978). G. Bilalbegović and N. M. Švrakić, J. Stat. Phys. **46**, 777 (1987); G. Bilalbegović, *ibid.* **50**, 1131 (1988).

[6]C. N. Yang, Phys. Rev. **85**, 809 (1952); G. F. Newell and E. W. Montroll, Rev. Mod. Phys. **25**, 353 (1953).

[7]G. L. M. Dassen, A. Kooiman, and J. M. J. van Leeuwen, Physica A **159**, 91 (1989).

[8]J. D. Weeks, G. H. Gilmer, and H. J. Leamy, Phys. Rev. Lett. **31**, 549 (1973).